Use of Directional Wigner Distribution for Identification of the Instantaneous Whirling Orbit in Rotating Machinery

Chong-Won Lee
Yun-Sik Han

Center for Noise and Vibration Control(NOVIC), Department of Mechanical Engineering
KAIST, Science Town, Taejon, 305-701, South Korea
Tel : 82-42-869-3016, Fax : 82-42-869-8220, E_mail : cwlee@hanbit.kaist.ac.kr

ABSTRACT

A vibration signal processing technique, which utilizes the directional Wigner distribution(dWD) defined with the forward and backward pass analytic signals, is applied to a laboratory rotor kit during run-up for identification of its instantaneous whirling orbit. The aliasing problem and the interference terms between the forward(positive) and backward(negative) frequency components can be avoided in the two types of dWDs calculated with the transformations of complex-valued signals to the forward and backward pass analytic signals. The experimental results indicate that the auto-dWD essentially tracks the shape and directivity of the instantaneous whirling motion, whereas the phase of the cross-dWD indicates its inclination angle. The shape and directivity index(SDI) is proposed and used to quantify the shape and directivity information of whirling motion.

Keywords : Directional Wigner distribution, Analytic signal, Hilbert transform, Backward whirl, Shape and directivity index.

1. INTRODUCTION

An anisotropic rotor system possesses the non-axisymmetric properties in its supporting stationary structure. The anisotropy in stiffness and damping of the support is known to produce elliptic whirl due to imbalance, which may be forward (the same direction as the rotor rotation) or backward (the opposite direction to the rotor rotation) [1,2]. With light damping, the synchronous backward whirl often occurs when the rotor system is operated between two very closely spaced resonant speeds. It makes the shaft undergo two reversals in stress per revolution, so that it may significantly contribute to shaft fatigue. Consequently, in anisotropic rotor systems, it is important to identify the backward whirl between the two split critical speeds. One of the most common ways to check the synchronous whirling direction, is to run the rotor at a constant speed, while the rotor speed is incremented by a fixed amount. Thus it requires many repeated test runs. Another quick test method is the use of the automatically tuned filter to the rotor speed during run-up or coast down. However, as the sweep rate increases, the spectral bandwidth increases and the frequency resolution decreases. As an alternative, use of the Wigner Distribution of transient signal during run-up is proposed to identify the backward synchronous whirl including the shape and inclination angle of the whirl orbit. The Wigner distribution which conventionally deals with the real-valued time-varying signals is well documented in the literature [3-9]. Among others, the Wigner Distribution is known to have major drawbacks such as the aliasing problem, the nonpositivity property and the presence of interference terms. In this work, the auto- and cross-directional Wigner distributions (dWDs) are introduced to account for complex-valued time varying signals, which represent the planar motion of the measurement points in structures at each instant of time. The auto- and cross-dWDs are defined such that they carry the information on the shape and directivity, and the inclination angle, respectively, of the instantaneous planar motion. The dWD has the problems and remedies similar to the conventional Wigner distribution. The aliasing problem and the interference terms between the forward and backward harmonic components are avoided by transforming a complex-valued signal into the forward and backward pass analytic signals. The

reduction of the interference terms associated with multiple harmonic components and the elimination of possible negative values are achieved by convolving the dWD with a Gaussian window function.

2. COMPLEX NOTATION

In this section, we will establish the convention for representing complex signals and consider the complex harmonic components as phasors rotating in a complex plane[1,10-15].

Let us consider a pair of complex conjugate signals, $p(t)$ and $\overline{p}(t)$, of the form

$$p(t) = y(t) + \mathrm{j}z(t)\,,\quad \overline{p}(t) = y(t) - \mathrm{j}z(t)\,, \tag{1}$$

where $y(t)$ and $z(t)$ are the real signals, j ($=\sqrt{-1}$) means the imaginary number and the bar denotes the complex conjugate. It is then natural to associate the complex signal $p(t)$ with a moving point, or a moving vector drawn from the origin, in the plane whose Cartesian coordinates are $y(t)$ and $z(t)$, as indicated in Figure 1. The complex harmonic signal $p(t)$ of frequency ω can be rewritten in polar form, using Euler's formula, as

$$\begin{aligned} p(t) &= p^f(t) + p^b(t) \\ &= \left\{\frac{1}{2}(y_c + z_s) + \frac{\mathrm{j}}{2}(z_c - y_s)\right\} e^{\mathrm{j}\omega t} + \left\{\frac{1}{2}(y_c - z_s) + \frac{\mathrm{j}}{2}(z_c + y_s)\right\} e^{-\mathrm{j}\omega t}\,, \end{aligned} \tag{2}$$

where $p^f(t) = r^f e^{\mathrm{j}\omega t}$, $p^b(t) = r^b e^{-\mathrm{j}\omega t}$, $y(t) = y_c\cos\omega t + y_s\sin\omega t$, $z(t) = z_c\cos\omega t + z_s\sin\omega t$, $r^f = \left|r^f\right| e^{\mathrm{j}\theta^f}$, $r^b = \left|r^b\right| e^{\mathrm{j}\theta^b}$, the superscripts b and f denote the backward (clockwise) and forward (counter-clockwise in Figure 1), and, y_c and y_s (z_c and z_s) are the Fourier coefficients associated with $y(t)$ ($z(t)$). Note that the complex term $e^{\mathrm{j}\omega t}$ ($e^{-\mathrm{j}\omega t}$) is associated with the forward (backward) rotating unity vector at the circular rotating speed of ω and that the complex quantity r^f (r^b) is associated with the vector having the amplitude, $\left|r^f\right|$ ($\left|r^b\right|$), and the initial phase, θ^f (θ^b). The directivity and shape of the elliptic planar motion are determined as follows :

$$\begin{aligned} &r^f\,(r^b) = 0 \quad &:&\quad \text{backward (forward) circular planar motion,} \\ &\left|r^b\right| > \left|r^f\right| \quad &:&\quad \text{backward elliptic planar motion,} \\ &\left|r^b\right| = \left|r^f\right| \quad &:&\quad \text{straight line motion,} \\ &\left|r^b\right| < \left|r^f\right| \quad &:&\quad \text{forward elliptic planar motion.} \end{aligned} \tag{3}$$

To quantify the above shape and directivity information, we may introduce the shape and directivity index (SDI) defined as

$$-1 \le \mathrm{SDI} = \frac{\left|r^f\right| - \left|r^b\right|}{\left|r^f\right| + \left|r^b\right|} \le 1 \tag{4}$$

where the inequality relations can be easily proven. Note that

$$\begin{aligned} \mathrm{SDI} &= -1 \quad &:&\quad \text{backward circular planar motion,} \\ -1 < \mathrm{SDI} &< 0 \quad &:&\quad \text{backward elliptic planar motion,} \\ \mathrm{SDI} &= 0 \quad &:&\quad \text{straight line motion,} \\ 0 < \mathrm{SDI} &< 1 \quad &:&\quad \text{forward elliptic planar motion,} \\ \mathrm{SDI} &= 1 \quad &:&\quad \text{forward circular planar motion.} \end{aligned}$$

In other words, the sign of SDI determines the directivity and the absolute value of SDI indicates the roundness (the correlation coefficient to a circle). The inclination angle θ_{inc} of the ellipse made by the major axis of the ellipse with respect to the y axis is obtained as

$$\phi_{inc} = \frac{1}{2}(\phi^f + \phi^b). \tag{5}$$

Therefore, in order to identify the parameters of the elliptic planar motion, we need to acquire the shape, directivity, and inclination angle of planar motion.

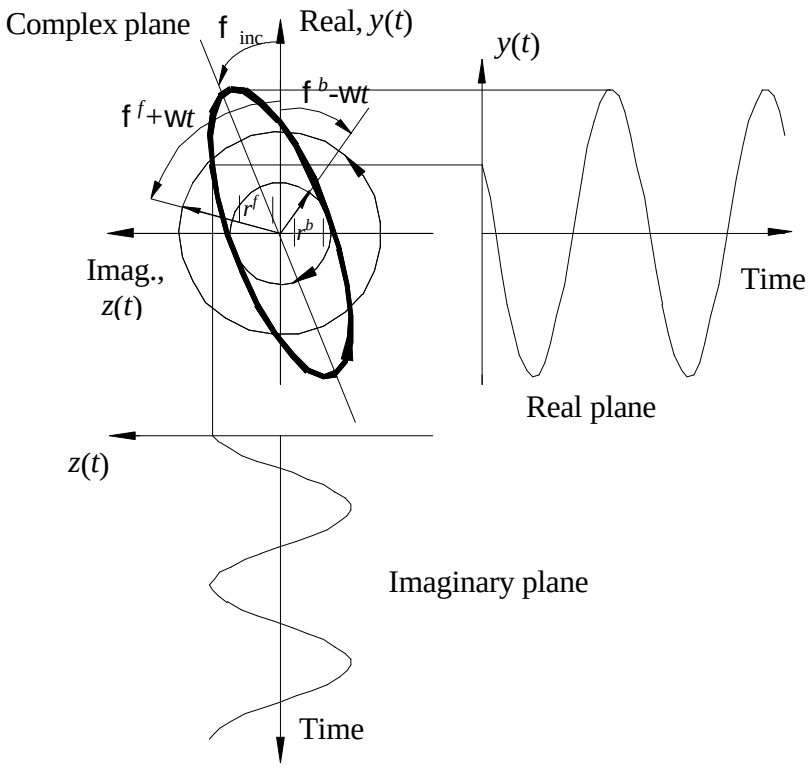

Figure 1 Representation of a complex-valued signal as the sum of two contra-rotating vectors

3. HILBERT TRANSFORM

3.1 DEFINITION

The conventional analytic signal associated with a real signal is defined such that the imaginary part is the Hilbert transform of the real signal, so that its spectrum is zero over the negative (backward) frequency region [16]. The use of conventional analytic signal can be considered as the forward pass transformation in the sense that it only passes the forward (positive) harmonic components. The backward pass transformation can be similarly designed by using the complex conjugate of the analytic signals. When we deal with real signals, the forward and backward pass transformations result in identical spectra except the sign of frequency. But the spectrum of a complex-valued signal, in general, shows the two-sided frequency contents, which are different over the positive and negative frequency ranges. Therefore, it is necessary to define the forward and backward pass analytic signals of a complex-valued signal.

Since the Hilbert transform is a linear operator, the Hilbert transform of a complex-valued signal $p(t)$ is another complex-valued signal $\tilde{p}(t)$, i.e.

$$\tilde{p}(t) = \int_{-\infty}^{\infty} \frac{p(u)}{\pi(t-u)} du \quad = p(t) * (1/\pi t). \tag{6}$$

3.2 ANALYTIC SIGNALS ASSOCIATED WITH COMPLEX SIGNALS

An analytic signal associated with a complex signal can be defined so that it consists of the complex-valued original signal and its Hilbert transformed signal. With a time signal $p(t)$ and its Hilbert transform $\tilde{p}(t)$, the forward and backward pass analytic signals, $p^f(t)$ and $p^b(t)$, associated with $p(t)$ can be defined as

$$p^f(t) = \{p(t) + \mathrm{j}\,\tilde{p}(t)\}/2\,,\quad p^b(t) = \{p(t) - \mathrm{j}\,\tilde{p}(t)\}/2\,. \tag{7}$$

Note that the forward (backward) pass analytic signal only includes the positive (negative) frequency components.

4. DIRECTIONAL WIGNER DISTRIBUTION

In this section, the conventional Wigner distribution is extended to account for complex signals by introducing dWD, and the properties of dWD are examined.

By simply replacing the real signal in the conventional definition of WD by the complex-valued signal, we may define the auto- and cross-WDs, $W_p(t,\mathrm{w})$ and $W_{\bar{p},p}(t,\mathrm{w})$ of a complex-valued signal $p(t) = y(t) + \mathrm{j}\,z(t) = p^f(t) + p^b(t)$ as [5]

$$\begin{aligned} W_p(t,\mathrm{w}) &= W_{p,p}(t,\mathrm{w}) = \int_{-\infty}^{\infty} \mathrm{e}^{-j\mathrm{w}t}\, \bar{p}(t-\frac{\mathrm{t}}{2})\, p(t+\frac{\mathrm{t}}{2})\mathrm{d}t\,, \\ &= W_{p^f,p^f}(t,\mathrm{w}) + W_{p^b,p^b}(t,\mathrm{w}) + W_{p^f,p^b}(t,\mathrm{w}) + W_{p^b,p^f}(t,\mathrm{w})\,, \end{aligned} \tag{8a}$$

$$\begin{aligned} W_{\bar{p},p}(t,\mathrm{w}) &= \int_{-\infty}^{\infty} \mathrm{e}^{-j\mathrm{w}t}\, p(t-\frac{\mathrm{t}}{2})\, p(t+\frac{\mathrm{t}}{2})\mathrm{d}t\,, \\ &= W_{\bar{p}^f,p^b}(t,\mathrm{w}) + W_{\bar{p}^b,p^f}(t,\mathrm{w}) + W_{\bar{p}^f,p^f}(t,\mathrm{w}) + W_{\bar{p}^b,p^b}(t,\mathrm{w})\,, \end{aligned} \tag{8b}$$

where $W_{p^f,p^f}(t,\mathrm{w})$ and $W_{p^b,p^b}(t,\mathrm{w})$ $\left(W_{\bar{p}^f,p^b}(t,\mathrm{w}) \text{ and } W_{\bar{p}^b,p^f}(t,\mathrm{w})\right)$ contain, in addition to the desired signal terms, the undesired interference terms between multi-harmonic components. On the other hand, $W_{p^f,p^b}(t,\mathrm{w})$ and $W_{p^b,p^f}(t,\mathrm{w})$ $\left(W_{\bar{p}^f,p^f}(t,\mathrm{w}) \text{ and } W_{\bar{p}^b,p^b}(t,\mathrm{w})\right)$ are the interference terms between the forward and backward harmonic components. Note that by definition, the Wigner kernels $\bar{p}(t-\frac{\mathrm{t}}{2})\,p(t+\frac{\mathrm{t}}{2})$ and $p(t-\frac{\mathrm{t}}{2})\,p(t+\frac{\mathrm{t}}{2})$ are the conjugate even and even functions of t, respectively. Especially, from definition (8), it holds

$$W_p(t,\mathrm{w}) = \overline{W_p}(t,\mathrm{w})\,, \tag{9a}$$

$$W_{\bar{p},p}(t,\mathrm{w}) = W_{\bar{p},p}(t,-\mathrm{w}) = \overline{W}_{p,\bar{p}}(t,\mathrm{w})\,. \tag{9b}$$

In other words, the auto-WD, which is the Fourier transform of the conjugate even Wigner kernel with respect to t, is real, but not always positive, whereas the cross-WD, which is the Fourier transform of the even Wigner kernel with respect to t, is an even, but not real in general, function of w.

On the other hand, the auto- and cross-dWDs of a complex-valued signal $p(t)$ are defined with the forward and backward pass analytic signals, respectively, as

$$dW_p(t,\mathrm{w}) = \begin{cases} \int_{-\infty}^{\infty} \mathrm{e}^{-j\mathrm{w}t}\, \bar{p}^f(t-\frac{\mathrm{t}}{2})\, p^f(t+\frac{\mathrm{t}}{2})\mathrm{d}t & ,\textit{for } \mathrm{w}>0, \\ \int_{-\infty}^{\infty} \mathrm{e}^{-j\mathrm{w}t}\, \bar{p}^b(t-\frac{\mathrm{t}}{2})\, p^b(t+\frac{\mathrm{t}}{2})\mathrm{d}t & ,\textit{for } \mathrm{w}<0, \end{cases} \tag{10a}$$

$$dW_{\bar{p},p}(t,\mathrm{w}) = \int_{-\infty}^{\infty} \mathrm{e}^{-j\mathrm{w}t}\, p^b(t-\frac{\mathrm{t}}{2})\, p^f(t+\frac{\mathrm{t}}{2})\mathrm{d}t \quad ,\textit{for all } \mathrm{w}, \tag{10b}$$

which state that by separating the backward or forward components, we can remove the interference terms between the forward and backward components. Thus, for complex-valued signals, the dWDs defined in equation (10) are far less contaminated by undesired interference terms than the WDs in equation (8). In addition, the dWD defined by using the analytic signal can eliminate the aliasing problem. On the other hand, the remaining interference terms of a multi-component signal can be reduced with the smoothed dWD, which is acquired by convolving the dWD with a Gaussian smoothing function in the time and frequency domain [17].

We can also define the instantaneous SDI of the time varying complex harmonic component, i.e.

$$-1 \le \mathrm{SDI}(t) = \frac{\left|r^f(t)\right| - \left|r^b(t)\right|}{\left|r^f(t)\right| + \left|r^b(t)\right|} \le 1, \tag{11}$$

where $\left|r^f(t)\right| = \sqrt{\frac{1}{2\pi}\int_{w_1}^{w_2} dW_p(t,w)dw}$, $\left|r^b(t)\right| = \sqrt{\frac{1}{2\pi}\int_{-w_2}^{-w_1} dW_p(t,-w)dw}$. Here w_1, w_2 form frequency band near a spectral peak of interest. The above integral of the auto-dWD over the finite frequency band $w_1 < w < w_2$, $-w_2 < w < -w_1$ is equal to the instantaneous signal power contained in the frequency band. Note that the implication of the above relation is similar to equation (4).

To demonstrate some important properties of auto- and cross-dWDs, we consider a complex chirp signal, whose instantaneous frequency increases linearly with time; i.e.

$$p(t) = r^f\, e^{jat^2/2} + r^b\, e^{-jat^2/2}, \tag{12}$$

where $r^f = \left|r^f\right| e^{j\theta^f}$, $r^b = \left|r^b\right| e^{j\theta^b}$. Here a is a constant. From equation (10a), we obtain the corresponding auto-dWD as

$$dW_p(t,w) = \begin{cases} 2\pi\left\{\left|r^f\right|^2 \delta(w - at)\right\} & , for\ w > 0 \\ 2\pi\left\{\left|r^b\right|^2 \delta(w + at)\right\} & , for\ w < 0 \end{cases}. \tag{13}$$

It implies that the auto-dWD of the complex chirp signal is concentrated at any instant around the instantaneous forward(positive) and backward(negative) frequencies, $+at$ and $-at$, respectively, in the time-frequency plane. This is one of the main motivations for its use. On the other hand, the cross-dWD becomes

$$dW_{\bar{p},p}(t,w) = 2\pi\left\{\left|r^f\right|\left|r^b\right| e^{j\theta^f} e^{j\theta^b}\left[\delta(w - at)\right]\right\}. \tag{14}$$

Note that the auto- and cross-dWDs remove the undesired interference term between the forward and backward components. The instantaneous inclination angle can be defined, from the phase of the cross-dWD, as

$$\tan\left\{2\theta_{inc}(t,w)\right\} = \frac{\mathrm{Im}\left\{dW_{\bar{p},p}(t,w)\right\}}{\mathrm{Re}\left\{dW_{\bar{p},p}(t,w)\right\}}. \tag{15}$$

Thus, the instantaneous inclination angle can be expressed as

$$\theta_{inc}(t,w) = \frac{1}{2}\left[\theta^f + \theta^b\right]. \tag{16}$$

5. EXPERIMENTAL SET-UP

Figure 2 is the schematic of the laboratory test rig (Bently Nevada rotor kit: Model 24755). The test rig consists of one rigid disk and two bearing support pedestals. The inboard pedestal contains bronze bushing. The outboard pedestal uses a preload frame to generate the stiffness asymmetry effect in the

rig. The lateral vibrations adjacent to the outboard pedestal are measured by a pair of eddy current type proximity probes. The rotor system is driven by an electric motor incorporated with the tacho feedback through a flexible coupling. The recorded signals are filtered prior to A/D conversion using the low-pass filters with a nominal cut-off frequency of 200 Hz, and then sampled at a rate of 400 Hz. Each data set consists of 1024 data points.

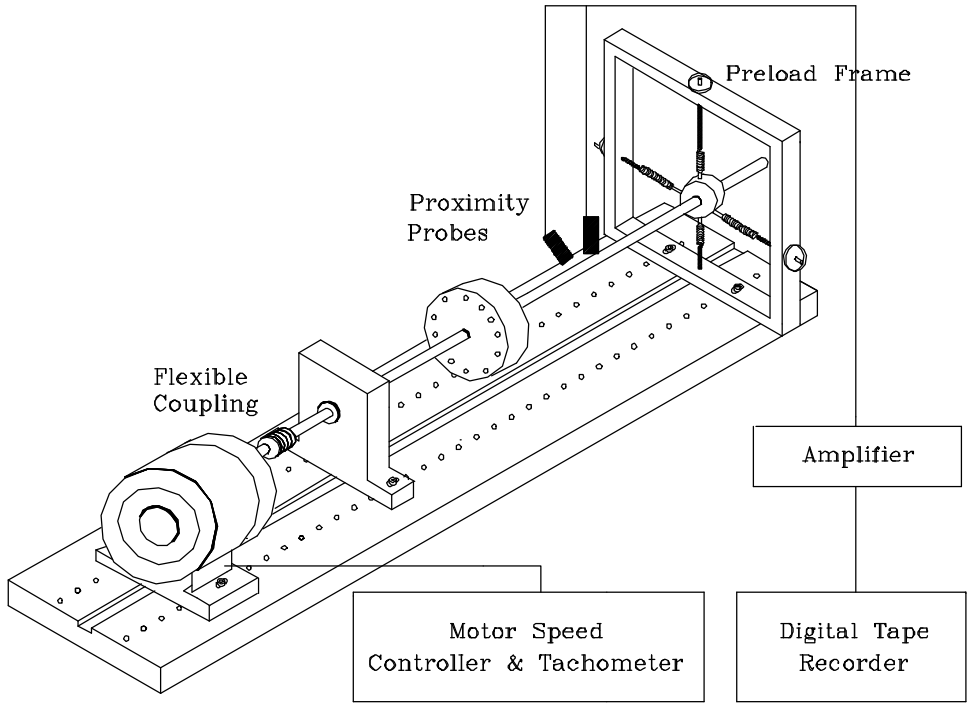

Figure 2 experimental setup for rotor run-up test

6. RESULTS AND DISCUSSION

Figure 3 shows the displacement time histories and the whirl orbits in the neighborhood of the two critical speeds, when the rotating speed of the rotor is swept up from 2200 rpm to 2460 rpm with a constant acceleration rate. The time histories show that the y-axis critical speed is lower than the z-axis critical speed, so that the y-displacement reaches its maximum amplitude first. Whirl orbits versus running time show the presence of the backward whirl between 0.7 sec and 1.75 sec. Especially, at about 0.7 sec running time, the orbits are collapsed into a straight line. At higher speeds, the whirl orbit begins to collapse again at about 1.75 sec. These events are necessary for the change of whirling direction from the continuity point of view. It can also be seen from the whirl orbits that the major axis of orbits become inclined increasingly from y-axis to z-axis.

Figure 4 shows the smoothed auto-dWD, and the instantaneous SDI and inclination angle of 1X (synchronous to the rotational speed) component. It can be seen that the smoothed auto-dWD in Figure 4 (a) well represents the time for backward whirl, its frequency components, and the shape of the instantaneous orbit. The smoothed auto-dWD shows that the two critical speeds are in the neighborhood of 2280 rpm and 2390 rpm, respectively. Note that Figure 4 in comparison with the whirl orbits as shown in Figure 3(c) shows the characteristics of instantaneous whirling orbits during run-up in detail. SDI in Figure 4 (b) clearly shows the shape and directivity of the instantaneous whirling orbit, and Figure 4(c) represents the instantaneous angle of 1X component made by the major axis of the orbits with y-axis. As shown in the time histories, response signals contain almost mono-component, that is, synchronous component, because the rotor operates at the neighborhood of critical speeds. Thus the

resulting smoothed dWDs have little effects of the interference terms between multiple harmonic components, and make interpretation effective.

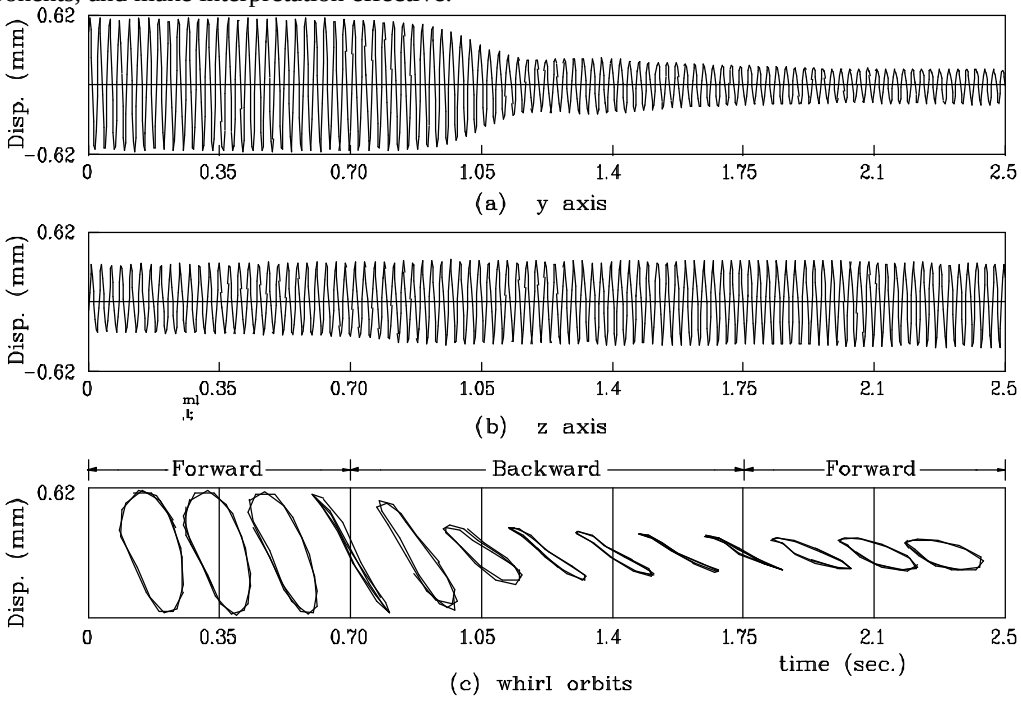

Figure 3 Vibration signals and whirl orbits during rotor run-up test

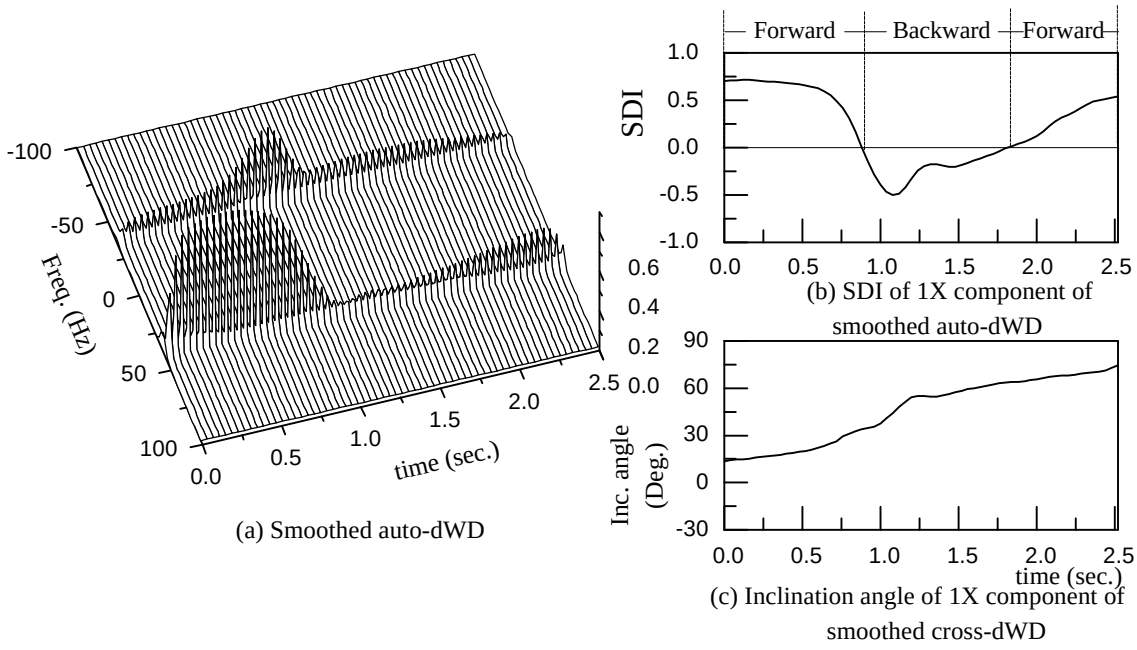

Figure 4 Rotor run-up test : f_s = 400 Hz, N=1024, smoothing window size = 20×20

7. CONCLUSION

Transient vibration signal processing method is developed utilizing the smoothed dWD of complex-valued signal representing the instantaneous planar motion. Two types of the smoothed dWDs are proposed : auto- and cross-dWDs. And the experimental result for identification of the instantaneous whirling orbit in rotor during run-up shows that the shape, directivity, and inclination angle of the instantaneous planar motion can be effectively identified by using the smoothed auto-and cross-dWDs, respectively.

ACKNOWLEDGMENT

The authors would like to acknowledge the support of the rotor kit from the Bently Nevada Corporation.

REFERENCES

1 Lee, C.W., *Vibration Analysis of Rotors*, Kluwer Academic Publishers (1993).

2 Joh, C.Y., and Lee, C.W., Use of dFRFs for Diagnosis of Asymmetry/Anisotropy Properties in Rotor-Bearing System, *ASME J. of Vibration and Acoustics*, Vol.118, Jan (1996) 64-69.

3 Cohen, L, *Time-Frequency Analysis*, Prentice Hall (1995).

4 Qian, S. and Chen, D., *Joint Time-Frequency Analysis*, Prentice Hall (1996).

5 Claasen, T.A.C.M., and Mecklenbrauker, W.F.G., The Wigner distribution- A Tool for Time-Frequency Signal Analysis, *Philips Journal of Research*, Vol.35 (1980) Part I:217-250, Part II: 276-300, Part III: 372-389.

6 Hlawatsch, F., and Boudreaux-Bartels, G.F., Linear and Quadratic Time-Frequency Signal Representations, *IEEE Signal Processing Magazine*, Vol.9, No. 2 (1992) 21-67.

7 Meng, Q., Qu, L., Rotating Machinery Fault Diagnosis Using Wigner distribution, *Mechanical Systems and Signal Processing*, Vol.5(3) (1991) 155-166.

8 Leuridan, J., Auweraer, H.V.D., Vold, H., The Analysis of Nonstationary Dynamic Signals, *Sound and Vibration*, Aug. (1994) 14-26.

9 Shin, Y.S., Jeon, J.J., Pseudo Wigner-Ville Time-Frequency Distribution and Its Application to Machinery Condition Monitoring, *Shock and Vibration*, Vol.1, No. 1 (1993) 65-76.

10 Lee, C.W., Park, J.P., and Han, Y.S., Use of Directional AR and ML Spectra for Detection of Misfired Engine Cylinder, *Fifteenth Biennial ASME Conference on Vibration and Noise*, Vol. 3, Part A, DE-Vol. 84-1 (1995) 1397-1403.

11 Lee, C.W., Joh, Y.D., A New Horizon in Modal Testing of Rotating Machinery, Keynote Paper, *The Fourth Asia-Pacific Vibration Conference*, Melbourne, November (1991)

12 Lee, C.W., Joh, C.Y., Use of Directional Spectra for Diagnosis of Asymmetry/Anisotropy in Rotor Systems, *Fourth International Conference on Rotor Dynamics*, Chicago, Sep. (1994) 97-101.

13 Lee, C.W., Park, J.P., Inner Race Fault Detection in Rolling Element Bearings by Using Directional Spectra of Vibration Signals, *Sixth International Conference on Vibrations in Rotating Machinery*, Oxford, U.K., Sep. (1996) 361-370.

14 Lee, C.W., Han, Y.S., Transient Engine Vibration Analysis by using Directional Wigner Distribution, *SAE Noise and Vibration Conference*, Traverse City, May (1997).

15 Southwick, D., Using Full Spectrum Plots, *Orbit*, Vol.14, No.4, Dec. (1993) 19-21.

16 Randall, R. B., *Frequency Analysis*, B & K Co. Ltd., 3rd ed. (1987).

17 Hlawatsch, F., Manickam, T.G., Urbanke, R.L., Jones, W., Smoothed pseudo-Wigner distribution, Choi-Williams distribution, and cone-kernel representation: Ambiguity-domain analysis and experimental comparison, *Signal Processing*, Vol.43 (1995) 149-168.

NOMENCLATURE

$dW_p(t,\omega)$ ($dW_{\bar{p},p}(t,\omega)$)	Auto- and cross-directional Wigner Distribution of a complex-valued signal
$p(t)$	Complex-valued lateral deflection ($y(t) + jz(t)$)
$p^f(t)$ ($p^b(t)$)	Forward(backward) pass analytic signal
$\tilde{p}(t)$	Hilbert transformed lateral deflection of a complex-valued signal $p(t)$
r^f (r^b)	Forward(backward) rotating vector with the amplitude $\left\|r^f\right\|$ ($\left\|r^b\right\|$), and the initial phase, ϕ^f (ϕ^b).
SDI	Shape and directivity index
t	Time
$W_p(t,\omega)$ ($W_{\bar{p},p}(t,\omega)$)	Auto- (cross-) Wigner Distribution of real signal
$y(t)$, $z(t)$	Rotor lateral defections in two orthogonal directions
y_c , y_s (z_c , z_s)	Fourier coefficients associated with $y(t)$ ($z(t)$) direction
ω	Circular frequency of the whirling orbit
ϕ_{inc}	Inclination angle of whirling orbit